JOURNAL OF MECHANICAL ENGINEERING AND SCIENCES (JMES)
ISSN: 2289-4659 e-ISSN: 2231-8380
VOL. 15, ISSUE 1, 7846 – 7859
DOI: https://doi.org/10.15282/jmes.15.1.2021.19.0619

ORIGINAL ARTICLE

Geometrical consideration for mechanical contact between rolling circle and surface roughness as an improvement to the surface profile

T. Shimizu[1], Y. Haramiishi[1], T. Ishii[1], Y. A. Rahim[2], M. F. A. Ahmad[3] and H. Watanabe[1]

[1] Faculty of Engineering, University of Yamanashi, Yamanashi 4008511, Japan
Phone: +81552208445; Fax: +81552208445
[2] Faculty of Mechanical Engineering Technology, Universiti Malaysia Perlis, Pauh Putra Campus, 02600 Arau, Perlis, Malaysia
[3] School of Engineering, Faculty of Science and Technology, Quest International University, Ipoh 30250, Malaysia

ABSTRACT – This paper describes measurement methods of surface profiles that improve contact-type displacement sensor outputs by focusing on the contact point between the sphere tip of the sensor and the rough surface. We examined the geometry of a surface profile model and compared measurements using various methods with the measurement using a roughness meter. The spherical tip of the contact type displacement sensor touches the measurement surface and detects the displacement. The sphere tip radius of a typical contact-type displacement sensor ranges from 1–3 mm, causing the roughness curve to be "filtered" by the radius of the sphere. Three methods for estimating the valley portion of the surface profile are evaluated in this study: a) linear approximation of the concave portion of the surface profile, b) function approximation of the concave portion, and c) using the known nose radius of the machining tool. The following sphere tip radii were used to measure actual surface profiles: 0.25 mm, 0.5 mm, 1.0 mm and 1.5 mm. Given the conditions of the experimental model, we found that surface profiles with a roughness that approximates a predictable curve can be measured with a high degree of accuracy.

ARTICLE HISTORY
Received: 27th July 2019
Revised: 27th July 2020
Accepted: 14th Oct 2020

KEYWORDS
Measurement; surface profile; roughness; surface topology; sphere tip radius; machine measurement

INTRODUCTION

Surface profiles consist of waviness and roughness [1]; these are important elements that impact the performance of mechanical parts. Hence, the shape and size of rough areas on a machined surface influence the performance of the final product. Many studies have examined the roughness of a machined surface. Corral et al. measured the surface roughness of a cylindrical honing finish using a cubic boron nitride (CBN) tool [2]. Heinrichs et al. examined the influence of tool materials and work pieces on roughness to investigate the characteristics of physical vapor deposition (PVD)-coated high speed steel (HSS) [3]. Fetecau et al. investigated the processing resistance and roughness when a turning process is used for Teflon (PTFE), with a polycrystalline diamond [4]. In ultra-precise diamond turning, influences of tool vibration on surface roughness [5], roughness evaluation of carbon fiber reinforced polymer (CFRP) using high-speed computer numerical control (CNC) cutting and robot arm trimming [6], and roughness measurement of carbon steel turning with wiper inserts [7] have been investigated. In addition to roughness, research has also focused on creating unique machined surfaces. Rendi et al. discussed machining a micro-dimpled pattern onto a material surface to improve the performance of mechanical parts. They developed a dual-frequency elliptical vibration texturing method and presented a theoretical surface roughness [8].

As described above, the evaluation of roughness is a key factor in the assessment of machined surfaces. However, the measurements of surface roughness are typically performed using a high-precision roughness meter in a temperature-controlled room. Currently, non-contact type systems such as laser microscopes employ one of the following methods to measure roughness: optical fiber [9], speckle [10], spectral reflectance [11], atomic force microscopy (AFM) [12], contrast of a speckled pattern [13], or interference optics [14]. However, the installation, handling, adjustment, and maintenance of the equipment required for these methods are costly and impractical.

For roughness estimation, a neural network method [15, 16] and the Monte Carlo method [17] were utilized to investigate the radius of the contact-type displacement gauge and the shape of the surface profile. Tomov et al. [18] considered two parameters for predicting surface roughness: a) kinematic-geometrical copying of the cutting tools onto the machined surface and b) distortion due to the influence of other cutting conditions. Shahabia and Ratnam used two-dimensional images of the nose area of tool tips to simulate the surface profiles of the specimen after turning was completed [19]. Zu and Zhan developed a multi-wavelength fiber sensor method that can measure surface roughness and surface scattering characteristics [20].

If such measurements could be performed with a contact-type displacement sensor such that the sensor output close to the surface profile, this high precision instrument could be used at the production site and would be an efficient, low-cost alternative to the methods listed above. Therefore, this study employs a contact-type displacement gauge to measure surface roughness. The measurement is performed by detecting the displacement when the sphere contacts the surface of

*CORRESPONDING AUTHOR | T. Shimizu | ✉ tsuyoshi-s@yamanashi.ac.jp

the object being measured. To measure the roughness by using a contact-type displacement gauge, it is necessary to clarify the geometrical relationship of the contact area between the sphere and the surface. The contact point between the surface and the sphere cannot be measured if the contact point (measurement point) is not directly below the center of the sphere, and the radius of curvature of the sphere is greater than that of the roughness. Therefore, a smaller sphere radius yields a more accurate measurement. However, commercially available contact-type displacement gauges have radii in the range of 1–3 mm, which is large compared with a roughness of several micrometers. Therefore, the contact type displacement gauge is often used as a sensor for measuring straightness rather than roughness. If the roughness is sufficiently small or the wavelength is sufficiently large, the surface profile can be estimated even if the radius of the sphere is somewhat large. The roughness wavelength of a machined surface is typically large. If the concavity cannot be measured and the sphere radius is sufficiently small, the concavity can be estimated by function approximation (FA) of the surface roughness.

Based on these assumptions, the geometry between the surface profile and the sphere tip is examined to determine whether the roughness height can be determined practically and accurately using a contact-type displacement gauge. This paper proposes the following methods to measure the concave portions of a rough surface: a) linear approximation (LA), b) FA, and c) the known nose radius of the cutting tool (NRK). Estimation of the concave portion of the profile surface and the restoration ratio of the profile height are examined to evaluate these methods.

GEOMETRIC RELATIONSHIP BETWEEN SURFACE AND SPHERE TIP

Surface Measurement

This study examined the trajectory curve of the sphere tip center in relation to the surface roughness. The sphere tip is referred to as the rolling circle in Figure 1. Figure 1 depicts the measurement method of scanning an actual surface. Figure 1(a) shows a surface scanning of a curve with a large radius of curvature; Figure 1(b) shows an unmeasurable part of a surface curve. In both figures, the scanning measurement is performed from left to right, and the trajectory of the rolling circle center is measured as the displacement of the sensor output.

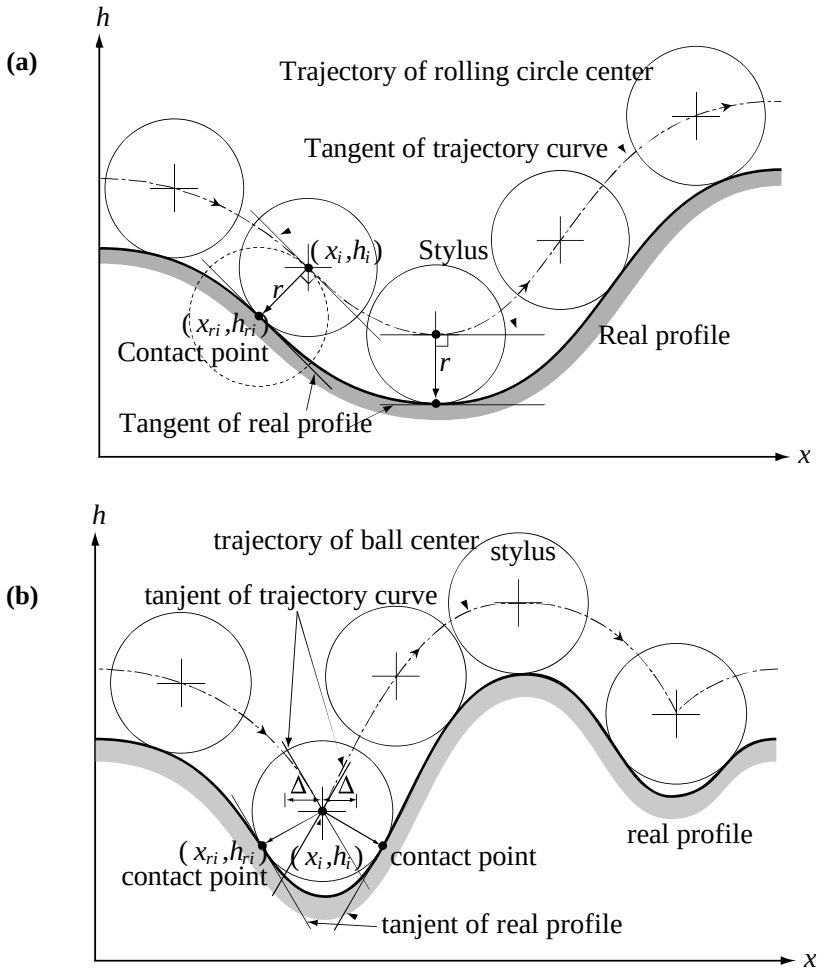

Figure 1. Measuring surface with ball stylus: (a) measurable profile and (b) unmeasurable profile

As shown in Figure 1(a), because the radius of the circle is less than the width of the concave portion of the surface, wecan accurately determine the surfaceprofile from the displacement of the sensor output. Here, the distance r between the trajectory of the rolling circle center and the actual profileremains constant. The tangent of the actual surface at the contact point (x_{ri}, h_{ri}) and the tangent at the trajectory of the circle center(x_i, h_i) are equal [a circle with radius *r*centered on the contact point (x_{ri}, h_{ri}) is in line with the trajectory of the center of the rolling circle (x_i, h_i)].

As the radius of the rolling circle is larger than the width of the concave portion, as shown in Figure 1(b), the circle cannot follow the bottom of the concave portion. Therefore, the actual surface cannot be geometrically measured. The trajectory of the rolling circle center is discontinuous, and the tangent ranges between x_i- D (D→0) and x_i+ D (D→0)at the rolling circle center (x_i, h_i). To calculate the roughness in this case, a method to estimate the distance to the bottom part of the roughness curve is required.

Measurement Condition of Bottom Shape

Figure 2 shows the geometric model of the minimum measurable roughness. The real surface depicts the smallest unit of the roughness curve and the rolling circle straddling the vertices B and C of the actual surface. The *x*-coordinate of the rolling circle center lies between B and C. Let Δh represent the difference in height between B and C and let lrepresent the wavelength between B and C in the measurement direction. The center of the rolling circle is at the intersection of the perpendicular bisector of BC and the trajectory of the rolling circle center; the distance from this intersection to BC is L. Let M be the interval between the *x*-coordinate of the rolling circle center and the *x*-coordinate of point P, that is, the midpoint of BC.

Assume thatthe height from the bottom of the rolling circle to B is h_0; hence, the following equations describe the geometric relationship:

$$L^2 = r^2 - \left(\frac{\sqrt{\lambda^2 + \Delta h^2}}{2}\right)^2 \tag{1}$$

$$M^2 = L^2 - \left(\frac{\Delta h}{2} + r - h_0\right)^2 \tag{2}$$

$$(r - h_0)^2 + \left(\frac{\lambda}{2} + M\right)^2 = r^2 \tag{3}$$

By rearranging these equations with $\Delta h << 1$, Eq. (4) can be derived:

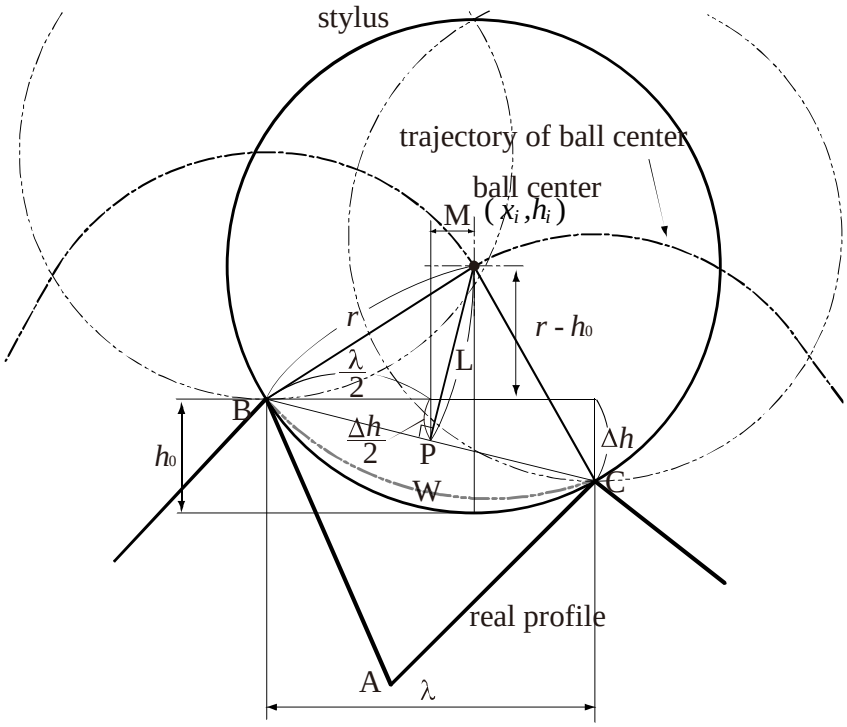

Figure 2. Geometric model of minimum measurable roughness

$$h_0{}^2 - (2r + \Delta h)h_0 + \frac{\lambda^2}{4} + r\Delta h = 0 \tag{4}$$

Therefore, considering $\lambda < 2r$ and $(\Delta h/2r)^2 \approx 0$, Eq. (4) becomes:

$$h_0 = r + \frac{\Delta h}{2} - r\sqrt{1 - \left(\frac{\lambda}{2r}\right)^2} \tag{5}$$

$$\text{where } \lambda < 2r \tag{6}$$

Roughness greater than this value cannot be measured. It is impossible to measure the bottom of the sphere. Therefore, if h_0 is the measurable maximum roughness (where the shape of the roughness concave portion A resembles the two-dot chain line W), measurements can be performed.

ESTIMATION OF ACTUAL SURFACE

The previous section mentions the measurability of an actual surface. As shown in Figure 2, if the rolling circle cannot be geometrically scanned, the roughness cannot be calculated unless the concave portion is estimated from the measurement results. A method for estimating surface concavity will be discussed in this section.

Linear Approximation of Concave Portion

Linear approximation method of the concave portion is defined as LA method in this paper. Figure 3 presents a model approximating the concavity of the surface with a straight line. The center of the rolling circle is point O, and the circle is in contact with the actual surface at points D and E, respectively. Let a and b be the angles between the trajectory of the rolling circle center at O and the vertical line passing through O, and let K be the intersection point of AD and the line parallel to AE passing through O. If the height of AD is L, Eq. (7) is obtained:

$$L = (\overline{AK} - \overline{KD})\cos\alpha \tag{7}$$

where

$$\overline{AK} = \frac{r}{\sin(\alpha + \beta)} \tag{8}$$

$$\overline{KD} = \frac{r}{\tan(\alpha + \beta)} \tag{9}$$

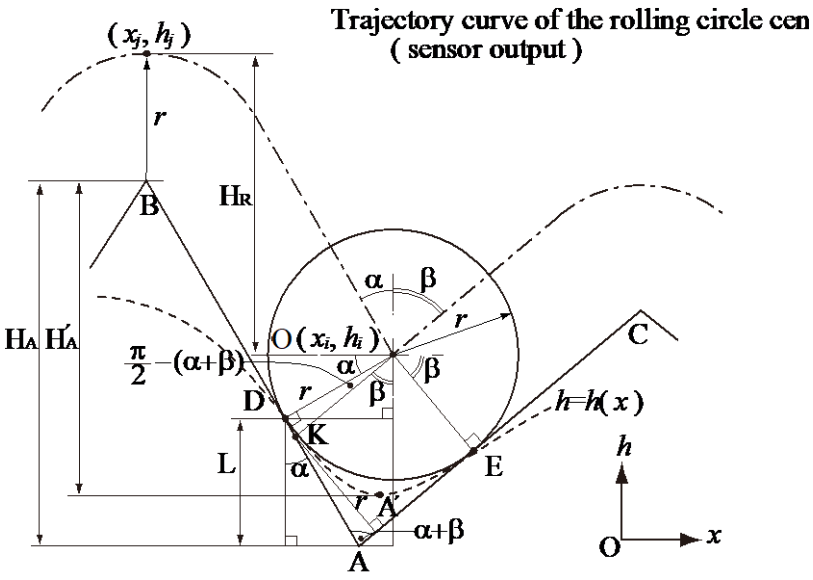

Figure 3. Collinear approximation of bottom of real surface

Therefore,

$$L = r\cos\alpha \frac{\cos(\alpha+\beta)+1}{\sin(\alpha+\beta)} \tag{10}$$

When the coordinates of point A are (x_A, h_A), Eq. (11) is obtained:

$$h_A = h_i - rsin\alpha - L \tag{11}$$

As a can be calculated from the trajectory of the rolling circle center, the equation of the straight line AD can be calculated as a straight line passing through the point D (x_D,h_D) = (x_i– r cos a,h_i – r sina) with the gradient tan(p/2 –a). Therefore, based on Eq. (11) and the equation of line AD:

$$x_A = \frac{h_A + tan(\pi/2-\alpha)(x_i - rcos\alpha) - (h_i - rsin\alpha)}{\tan(\pi/2-\alpha)} \tag{12}$$

Here, H_A can be written as:

$$H_A = \left(h_j - r\right) - (h_i - rsin\alpha - L) = h_j - h_i + r\frac{cos\alpha + cos\beta - sin(\alpha+\beta)}{sin(\alpha+\beta)} \tag{13}$$

Function Approximation of Concave Portion

In the previous subsection, the concave portion is approximated by a straight line. However, this section addresses FA. In Figure 3, $h(x)$ is the approximated function. As the rolling circle contacts the surface at points D and E, the following conditions apply:

(I) Line AD and line AE may be asymmetric at point O.

(II) The tangents at points D and E have the same slope as lines AD and AE.

$$h = ax^3 + bx^2 + cx^2 + d \tag{14}$$

It is necessary to choose a function that satisfies the above conditions. Therefore, a cubic functionisapplied: Assuming that the applied cubic function in Eq. (14) and the coordinates of point E are (x_E, h_E) = (x_i + r cos b, h_i−r sin$b$), parameters a, b, c, and d are expressed in a matrix as

$$\begin{bmatrix} {x_D}^3 & {x_D}^2 & x_D & 1 \\ {x_E}^3 & {x_E}^2 & x_E & 1 \\ 3{x_D}^2 & 2x_D & 1 & 0 \\ 3{x_E}^2 & 2x_E & 1 & 0 \end{bmatrix} \begin{bmatrix} a \\ b \\ c \\ d \end{bmatrix} = \begin{bmatrix} h_D \\ h_E \\ tan(2/\pi - \alpha) \\ tan(2/\pi - \beta) \end{bmatrix} \tag{15}$$

Therefore, the cubic function is determined by solving Eq. (15). Point A'= (x'_A, h'_A) (where $x_D \leq x'_A \leq x_E$) is determined by solving the derivative dh/dx = 0 of Eq. (14). Finally, we can calculate H_A as

$$H'_A = h_j - r - h'_A$$

In the case that the nose radius of the cutting tool is known

We define this method as the Nose Radius Known (NRK) method. Figure 4 shows the concave portion and the tool cutting edge. The nose radius of the tool is R, and the center coordinate of the circle of the cutting tool edge is O_T (c_x, c_h). Assume that the radius of the circle of the cutting tool edge is:

$$(x - c_x)^2 + (h - c_h)^2 = R \tag{16}$$

and the cutting tool edge is in contact with lines AD and AE at points P (x_P, h_P), and Q (x_Q, h_Q). If equations of AD and AE are:

$$h = sx + t \tag{17}$$

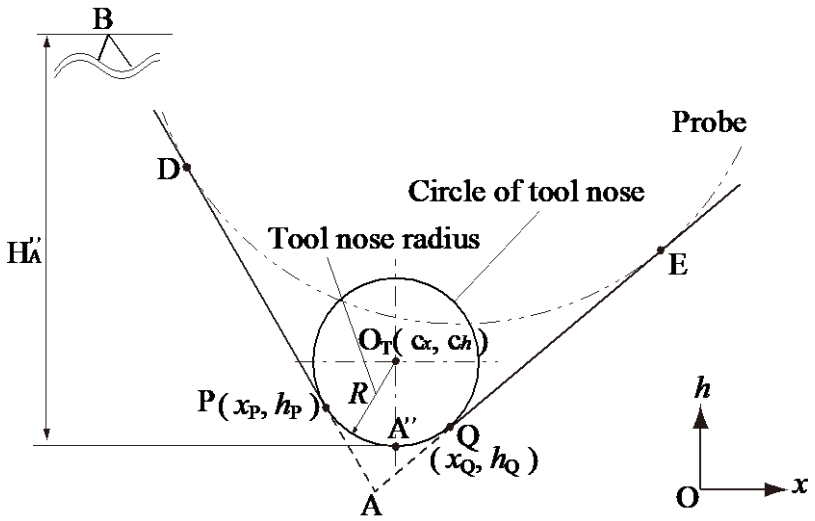

Figure 4. Considering the nose radius of the cutting tool

$$h' = s'x + t' \tag{18}$$

and the derivative of the cutting tool edge is d*h*/d*x*, the following Eq. (19) is obtained by examining the relationship between the circle of the tool nose and the contact point:

$$\left(\frac{dh}{dx}\right)^2 = \frac{\left(h_p - c_h\right)^2}{\left(x_p - c_x\right)^2} = \frac{\left(x_p - c_x\right)^2}{R^2 - \left(x_p - c_x\right)^2} = s^2$$
$$\Leftrightarrow x_p = c_x - \frac{R}{\sqrt{1+s^2}} \tag{19}$$

Similarly, h_P can also be calculated and found from Eq. (16) as:

$$h_p = c_h - \frac{sR}{\sqrt{1+s^2}} \tag{20}$$

Therefore, because point P is on line AD, Eq. (20) can be rewritten as:

$$sc_x - c_h = -t \tag{21}$$

Similarly, Eq. (22) can be obtained from the relationship between the equations of line AE and the edge circle of the cutting tool.

$$s'c_x - c_h = -\frac{2s'^2R}{\sqrt{1+s'^2}} - t' \tag{22}$$

The simultaneous Eqs. (21) and (22) provide the point O_T. Hence, point A" is estimated as A" (c_x,c_h – R). Finally, we can calculate H"$_A$ as

$$\mathrm{H''}_A = h_j - r - (c_h - R). \tag{23}$$

EXPERIMENT

Experimental Setup

Experimental devices

Figure 5 depicts the experimental setup used in this study, and Table 1 lists the equipment specifications. The machinetool used in this study was a MAC-V05 manufactured by Takizawa Machine Tool Co., Ltd., the displacement gauge was model 80SB made by Tokyo Seimitsu Co., Ltd., and the roughness meter was model SE-3A manufactured by Kosaka Laboratory Ltd.. The specimen was placed on the table of the machining tool, and the measurement was made when the commercially contact type displacement sensor was fixed to the shank of a spindle. For comparison purposes, a cross section curve is obtained using a roughness meter. Figure 6 shows the 80SB displacement gauge with a stylus

radius of 1.5 mm, a stroke of 3 mm, and a measuring range of ±1100 mm. We can remove and replace the stylus tip to change the radius. Styluses used for measurement are shown in Figure 7 with the following radii: 0.25 mm, 0.5 mm, and 1.0 mm.

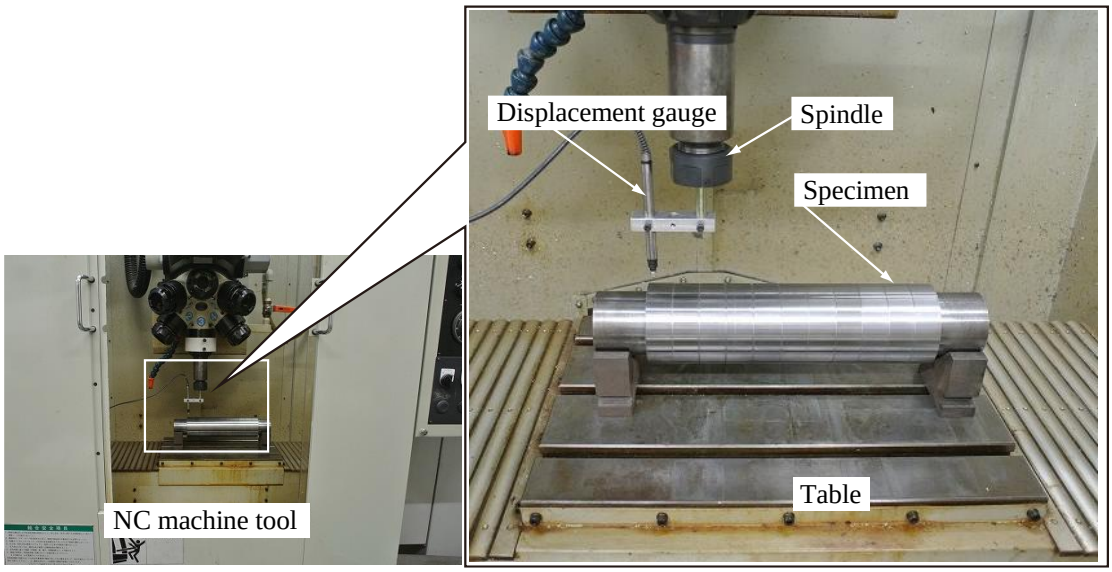

Figure 5. Machine tool (MAC-V05, Takisawa)

Table 1. Specifications of experimental setup

Equipment	Specifications
Machine tool	MAC V05, Takizawa Machine Tool 320 × 240 × 240(XYZ) BT30
Displacement gauge	80SB, Tokyo Seimitsu Stylus radius 1.5mm, stroke 3mm measuring range ±1100μm
Surface measuring instrument	SE-3A, Kosaka Laboratory stylus radius 2μm straightness accuracy 0.3/100 (μm/mm) measuring force 0.07N

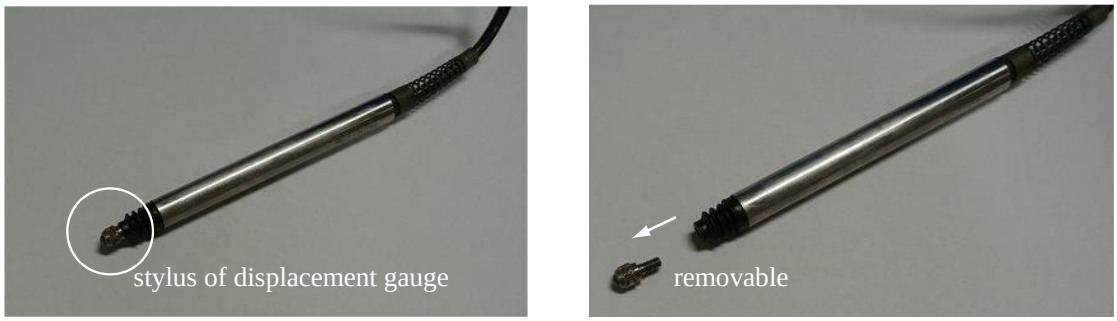

Figure 6. Displacement gauge

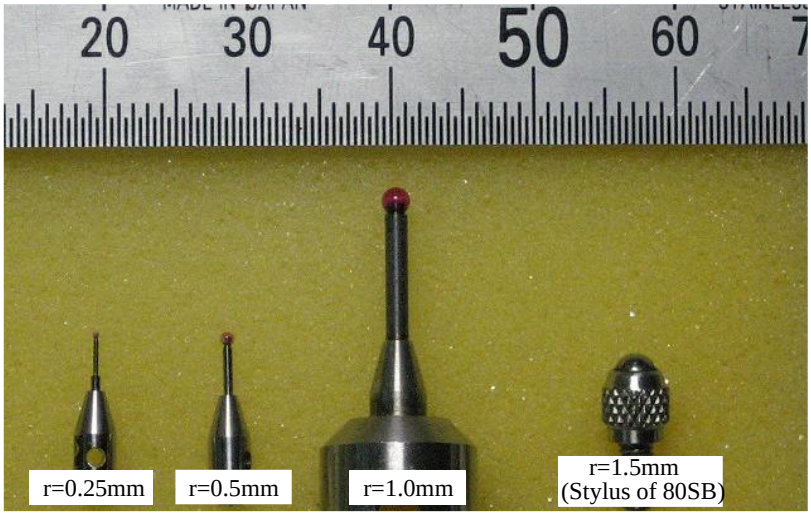

Figure 7. Styluses for measuring experiments

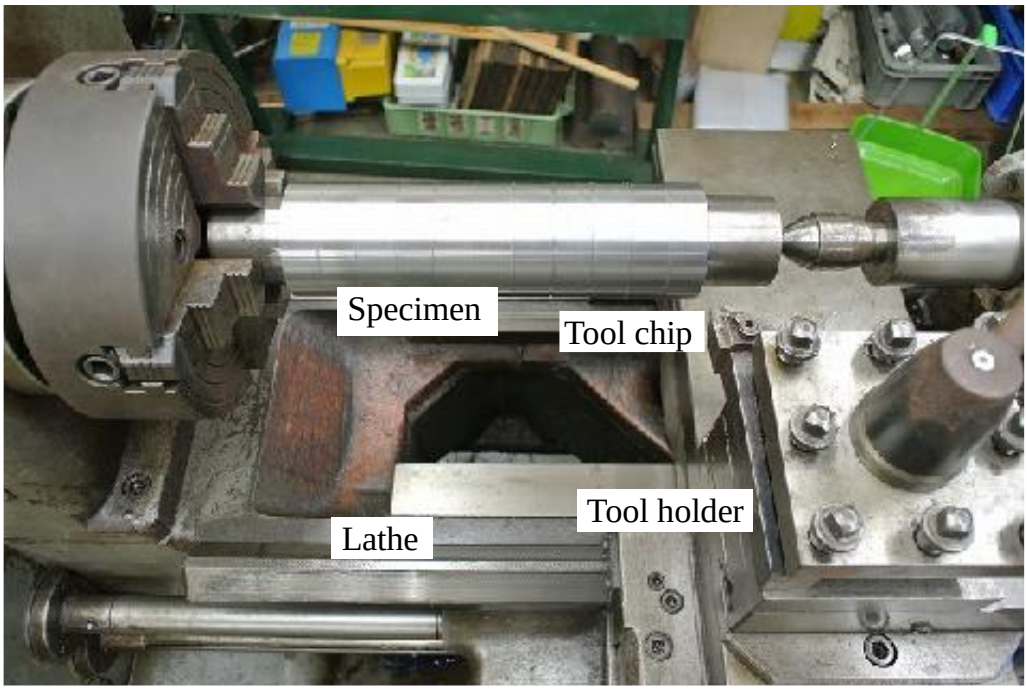

Figure 8. Making of specimens

Measurement specimens

Specimens were made using a lathe to control the surface roughness. Figure 8 shows a photograph of a specimen being created. The lathe used here is model TSL-800(Takisawa Co., Ltd.). The tool nose radius is 0.4 mm, and the cut depths are 0.2mm and 0.5 mm; the feed rates are 0.10, 0.15, 0.20, 0.25 and 0.26mm/rev. The rotation speed of the spindle is 1080 min^{-1}. Five measurement areas were created for each condition. The specimens are shown in Figure 9.

Experimental Results of Surface Measurement

To validate our proposed method, the turning surface was measured via a contact-type displacement sensor. The specimen was placed on the machine tool table described in the previous section. The displacement sensor was installed on the spindle of the machine tool, and the stylus contacted the specimen surface. To measure the surface of the specimen, G-code and M-code programs were executed and the sampling frequency of the A/D signal transformation (sensor output) was adjusted to the feed rate of the machine tool.

Figure 10 shows the measurement results of the turning surface with a cut depth of 0.2 mm and a 0.25mm/rev feed rate. Parameter *r* is the stylus radius. It appears more difficult to measure the surface accurately with a large radius.

Figure 11 is an enlarged view of the Local Windowin Figure 10. Measurement results for each stylus radius are shifted for comparison purposes. The wavelength is 0.285±0.014 mm.

Figure 9. Specimens

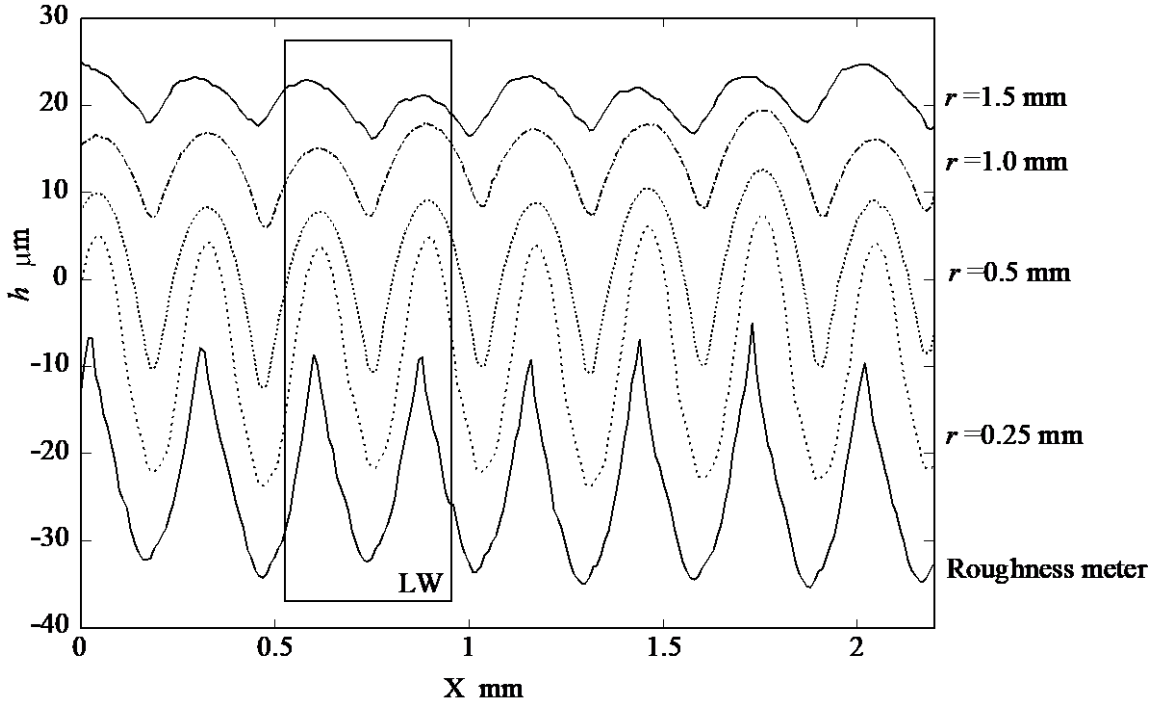

Figure 10. Measurements of the turning surface with different stylus radii

In Figure 11, it can be seen thatasthe stylus radius *r* increases, the stylus cannot scan the bottom. On the contrary, the profile attained using the sharp stylus tip can be measured accurately. The stylus with radius *r*=1.5 mm is unable to scan the height of the surface profile.

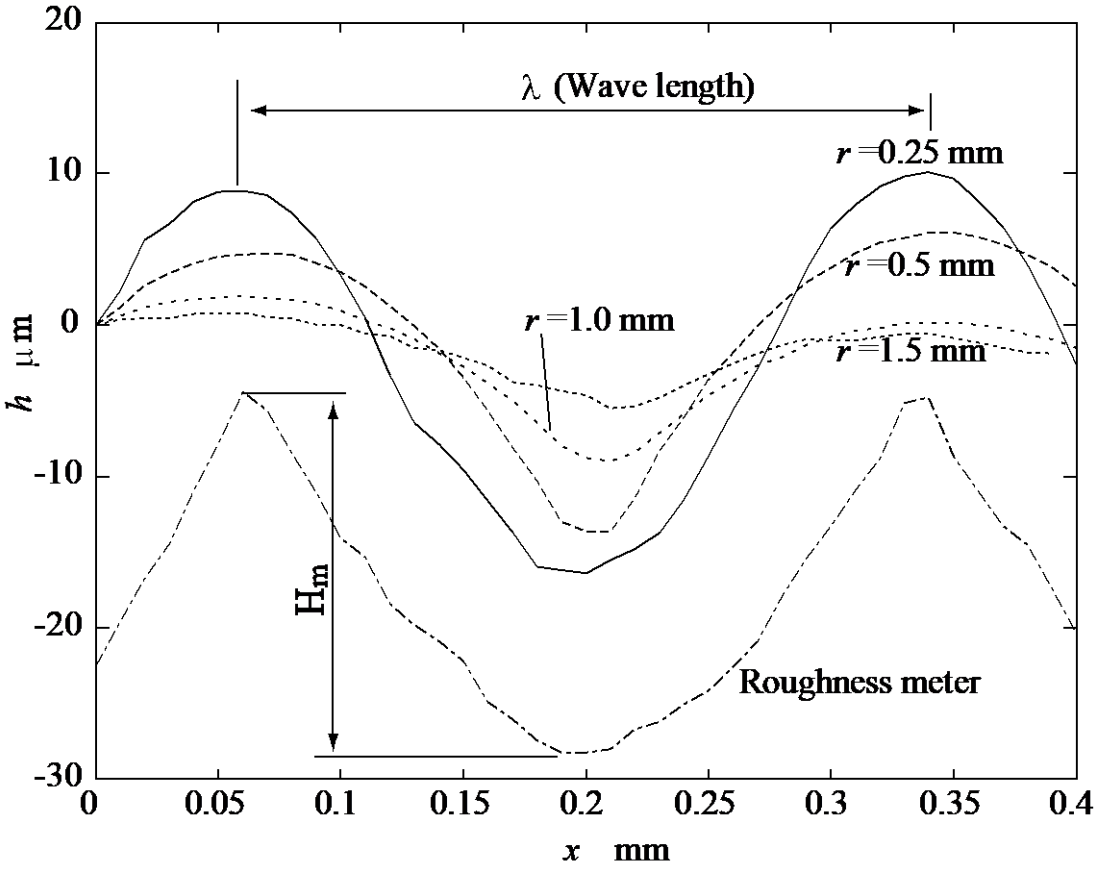

Figure 11. Measurement profile for each stylus

The measurement results are summarized in Table 2. H_m is the profile height measured with the roughness meter and is 26.0 ± 2.1 mm, and H_A is the height measurement using the LA method described in Section 3. H'_A and H''_A result from the FA and NRK methods, respectively. H_A is larger than H_r in all cases. We find it difficult to estimate the bottom of the profile in the case of r=1.5 mm. Therefore, we used styluses with radii of 0.25mm, 0.5mm, and 1.0mm.

Measurements of all specimens are shown in Figure 12. As the wavelength and stylus radius increase, the accuracy of the estimate of the concave portion decreases. When the wavelength is less than approximately 0.15 mm, the estimate approaches H_r.

Table 2. Measurement estimation results for each stylus radius

Stylus radius mm	H_r μm	H_A(LA) μm	H'_A(FA) μm	H''_A(NRK) μm
0.25	26.8 ±1.0	32.3±2.6	27.8±1.6	24.8±1.4
0.50	19.9±1.4	29.2±1.9	20.0 ±1.4	21.7±1.4
1.00	9.8±1.2	14.7±1.2	9.8±1.2	12.7±1.2
1.50	6.7±3.3	8.00±2.3	6.7±3.3	7.6±2.5

Roughness meter: 26.0 ± 2.1 μm

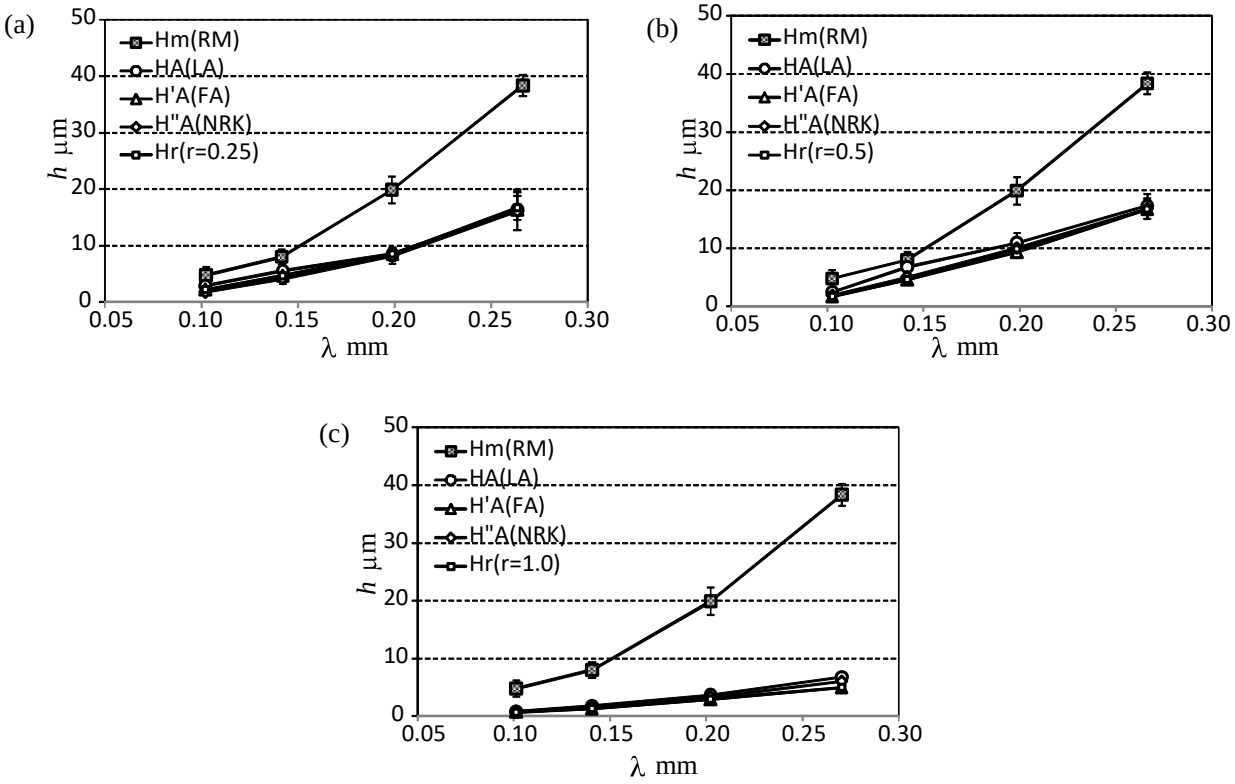

Figure 12. Measurements of all specimens: (a) stylus radius r=0.25mm, (b) r=0.5 mm and (c) r=1.0 mm

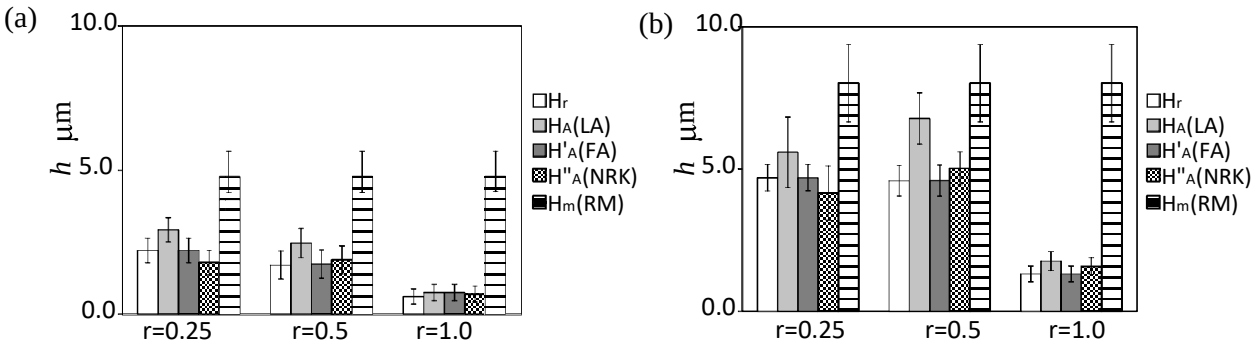

Figure 13. Detailed bar graph: Measurement of surface profile a) wavelength λ=0.102±0.025mm; b) λ=0.141±0.022mm

Discussion

Estimation of measurement results

To discuss the estimates in additional detail, we consider the case of λ=0.102mm and λ= 0.141 mm. Figure 13 shows a bar graph for λ = 0.102 mm (standard deviation=0.025mm) and 0.141 mm (standard deviation=0.022 mm).

In all cases, the LA method yielded a higher value than H_r and approaches the roughness meter measurement. The FA method yields a value equivalent to H_r, and the NRK method results in a value slightly less than or equal to H_r. Therefore, the LA method exhibits superior performance over the other proposed methods.

We proceeded to examine the LA results in more detail. When λ= 0.141, 85% of the height measurement is restored at r = 0.5 mm. In the case of r = 1.0 mm, approximately only 20% is restored for all methods. Therefore, the maximum optimal stylus radius r = 0.5 mm.

When comparing measurements for r = 0.25 mm and r = 0.5 mm, the standard deviation is high. In the case of the LA method, the intersection of the straight line approximating using the bottom of the profile is calculated, but the straight line is calculated by the least squares methodusing data of bottom profile. We consider that it depends on the linearity of the points of bottom profile, because least squares method is greatly affected by data with large outliers. Further study is recommended for devising an evaluation method based on the shape of the bottom.

Measurement results and measurement condition

Measurements using styluses with different radii are discussed above. The relationship between the stylus radius and measurement condition is investigatedhere.Figure 14 shows measurement conditions given in Section 2. Each h_0 curve is derived from Eq. (5), and stylus radii are 0.25 mm, 0.5 mm, and 1.0 mm. Figure14 shows the measurable maximum height for each stylus radius. The upper side of each curve is the unmeasurable range area (N), and the lower side is the measurable range area (P). Specimen wavelengths are indicated with bands measuring 0.102±0.025 mm, 0.141±0.022 mm, 0.200±0.017 mm, and 0.267±0.038 mm. In addition, profile heights of specimens are given from (I) to (IV). Regions (I) and (II) have P-regions for the h_0 (r = 0.25 mm) curve, however have small N-regions for the h_0 (r = 0.5 mm) curve. In addition, these region (I) and (II) have values close to H_r with r=0.25 mm and 0.5 mm. Regions (I) to (IV) have larger N-regions for the h_0 (r = 1.0 mm) curve. Therefore, restoration rates of regions (III) and (IV) with h_0 (r=1.0 mm) are low. From Figure 14, we see that the restoration rate is higher in regions (I) and (II) than in the other cases (even at r = 0.5 mm) because these regions are close to h_0 (r = 0.5 mm).

The restoration rate decreases as it deviates from theh_0 curve when measured with each stylus radius. However, even in the N-region, if the distance to h_0 is close, the restoration rate does not drop considerably. For conditions (II) and (III), the restoration rate using LA is high, andthe maximum restoration ratio is 48% at (III) for r=0.5 mm using LA.In the case of r = 0.25 mm, the value is almost the same as H_r. Overall, the average improvement was 21% compared with before the application of LA method.

Based on the observations above, it can be said that if the wavelength of the profile is short, the height of the profile can be restored if it is in the vicinity of the measurable boundary line in Figure 14.

Prediction of the profile height

We tested three samples to predict profile height with the LA method because this method performed better than the other proposed methods. Sample conditions are shown in Table 3. The conditions of (1) and (2) are turning, and the tool feed and cut depth are adjusted accordingly. The condition of (3) is milling.

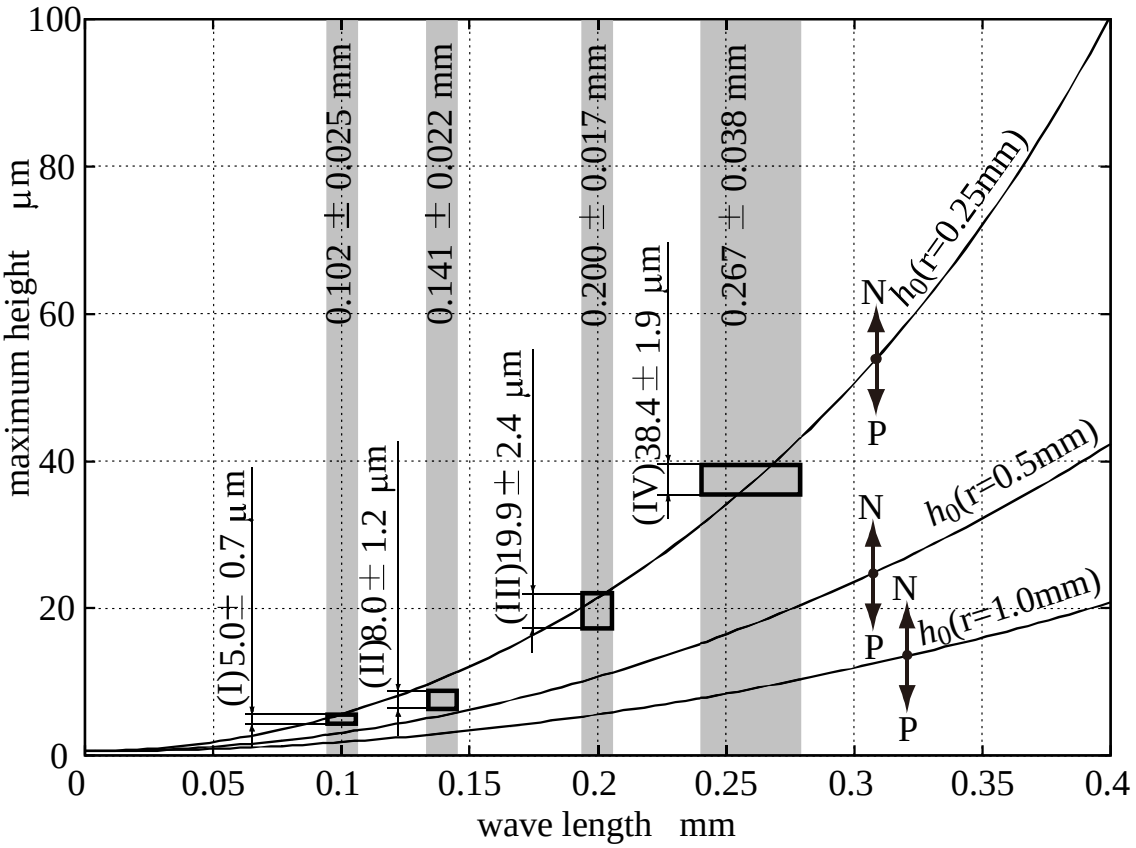

Figure 14. Measurable condition of each stylus and wave length of measuring profile

Table 3. Conditions of prediction experiment

No		Conditions
(1)	cutting	Turning / Feed rate 0.157 mm/rev / Nose radius of tool 0.4 mm/ Turning speed 80 m/min / depth of cut 0.2 mm
	measuring	Measuring with stylus radius 0.25mm
(2)	cutting	Turning / Feed rate 0.25 mm/rev, Nose radius of tool 0.4 mm/ Turning speed 80 m/min / depth of cut 0.2 mm
	measuring	Stylus radius 0.5 mm
(3)	cutting	Milling / Pick feed 0.2 mm / Nose radius of tool 0.8mm / Rotational Speed 2200 min^{-1} / Depth of cut 0.1 mm
	measuring	Stylus radius 0.5 mm

Measurement with the roughness meter and the displacement gauge are shown in Figure 15. In addition, estimated point A and vertex B of the displacement gauge output are connected with a line. It can be seen that the bottom of the displacement meter output approaches the bottom of the roughness meter output. Table 4 summarizes the estimation results of sample measurements. The prediction improves as the roughness decreases. Moreover, the closer to the judgment curve, the better is the prediction. Prediction is possible with a restoration rate of 80% or more.

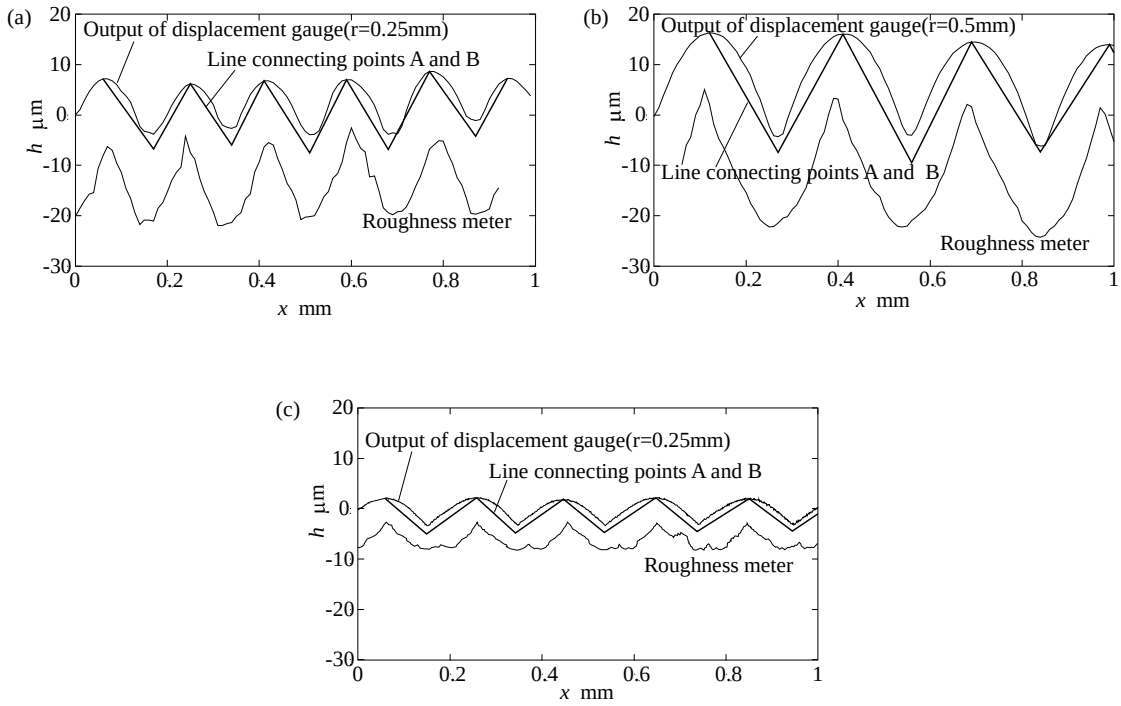

Figure 15. Experimental results: (a) condition (1), (b) condition (2), and (c) condition (3)

Table 4. Total results

No.	Hm(RM) μm	Hr μm	HA(LA) μm
(1)	16.1±1.3	10.2±1.2 (63.3%)	13.4±1.2 (83.2%)
(2)	26.6±2.5	20.1±1.6 (75.6%)	22.5±1.4 (84.6%)
(3)	5.8±0.2	5.1±0.3 (87.9%)	6.0±0.4 (103.4%)

CONCLUSION

This study investigated methods to improve the accuracy of surface profile measurement using a contact-type displacement sensor, considering the geometric relationship between the surface profileand the rolling circle radius. The methods evaluated included LA, FA, and varying the nose radius of cutting tools. In addition, the measurable range of each stylus radius wasderived, and the curves of theoretical ranges are shown. As a result, we arrived at the following conclusions: If the surface profile has a roughness height close tothe measurable condition curve, it is possible to predict the profile with high restoration. The LA method has the highest restoration ratefor the given conditions. Future studies can explore more precise statistical predictionssuch as using Machine Learning to determine the shape of surface profiles.

REFERENCES

[1] Geometrical Product Specifications (GPS) -Surface texture: Profile method -Terms, definitions and surface texture parameters, ISO Standard ISO4287:1997, 1997.

[2] I. B. Corral and J. V. Calvet. , "Roughness variability in the honing process of steel cylinders with CBN metal bonded tools," Precision Engineering, vol. 10, no. 35, pp.289-293, 2011.

[3] J. Heinrichs, J.Gerth, etal. , "Influence from surface roughness on steel transfer to PVD tool coatings in continuous and intermittent sliding contacts," Tribology International, vol. 56, pp. 9-18, 2012.

[4] C. Fetecau and F. Stan, "Study of cutting force and surface roughness in the turning of polytetrafluoroethylene composites with a polycrystalline diamond tool," Measurement, vol. 45, no. 6, pp. 1367-1379, 2012.

[5] H. Wang, S. To, C. Y. Chan, "Investigation on the influence of tool-tip vibration on surface roughness and its representative measurement in ultra-precision diamond turning," Int. J. Machine Tools & Manufacture, vol. 69, pp. 20-29, 2013.

[6] M. Slamani, S. Gauthier and J. F. Chatelain, "Comparison of surface roughness quality obtained by highspeed CNC trimming and high speed robotic trimming for CFRP laminate," Robotics and Computer-Integrated Manufacturing, vol. 42, pp. 63-72, 2016.

[7] A. E. Correia, J. P. Davim, "Surface roughness measurement in turning carbon steel AISI 1045 using wiper inserts," Measurement, vol. 44, no. 5, pp.1000-1005, 2011.

[8] R. Kurniawana, G. Kiswantob and T. J. Koa, "Surface roughness of two-frequency elliptical vibration texturing (TFEVT) method for micro-dimple pattern process," Int. J. Machine Tools & Manufacture, vol. 116, pp. 77-95, 2017.

[9] Y. Quinsat and C. Tournier, "Insitu non-contact measurements of surface roughness," Precision Engineering, vol. 36, no. 1, pp. 97-103, 2012.

[10] Z. Gao and X. Zhao, "Roughness measurement of moving weak-scattering surface by dynamic speckle image," Optics and Lasers in Engineering, vol. 50, no. 5, pp.668-677, 2012.

[11] I. Massoudi, M. M. Habchi, A.Rebey and B. E. Jani, "Study of surface roughness using spectral reflectance measurements recorded during the MOVPE of InAs/GaAs hetero structures," Physica E: Low-dimensional Systems and Nanostructures, vol. 44, no.7, pp. 1282-1287, 2012.

[12] P. D. Antonio, M. Lasalvia, G. Perna and V. Capozz. "Scale-independent roughness value of cell membranes studied by means of AFM technique," Biochimica et Biophysica Acta (BBA) - Biomembranes, vol. 1818, no.12, pp. 3141-3148, 2012.

[13] L. Tchvialeva, I. Markhvida and H. Zeng etal. , "Surface roughness measurement by speckle contrast under the illumination of light with arbitrary spectral profile," Optics and Lasers in Engineering, vol. 48, no. 7, pp. 774-778, 2010.

[14] H. Guo, L. Liu, X. Hao, K. Niu and X. Chou, "Profile measurement system based on linnik-type interferometric microscope for visible-light region and infrared-light region," Optics & Laser Technology, vol. 43, no.7, pp. 1184-1189, 2011.

[15] I. Asiltürk and M. Çunkaş, "Modeling and prediction of surface roughness in turning operations using artificial neural network and multiple regression method," Expert Systems with Applications, vol. 38, no.5, pp.5826-5832, 2011.

[16] F. J. Pontes, A. P. Paiva, P. P. Balestrassi, J. R. Ferreira and M. B. Silva, "Optimization of Radial Basis Function neural network employed for prediction of surface roughness in hard turning process using Taguchi's orthogonal arrays," Expert Systems with Applications, vol. 39, no. 9, pp. 7776-7787, 2012.

[17] T. Ghosh and S. Chattopadhyay, "A Monte Carlo simulation to study the effect of surface roughness on the performance of RPC," Nuclear Instruments and Methods in Physics Research, vol. 661, pp. S177- S181, 2012.

[18] M. Tomov, M. Kuzinovski and P. Cichosz, "Modeling and prediction of surface roughness profile in longitudinal turning," Journal of Manufacturing Processes, vol. 24, pp.231-255, 2016.

[19] H.H. Shahabia and M.M. Ratnam, "Simulation and measurement of surface roughness via grey scale image of tool in finish turning," Precision Engineering, vol. 43, January, pp. 146-153, 2016.

[20] Z. Nan-nan and Z. Jun, " Surface roughness measurement based on fiber optic sensor," Measurement, vol.86, May, pp. 239-245, 2016.